# Joint Centre for Mesoscale Meteorology, Reading, UK

## Parametrization of diabatic processes in the inversion of the omege-equation

M. Athanassiadou
A. J. Thorpe

Internal Report No. 60

June 1996

**Met Office** Joint Centre for Mesoscale Meteorology Department of Meteorology
University of Reading PO Box 243 Reading RG6 6BB United Kingdom
Tel: +44 (0)118 931 8425 Fax: +44 (0)118 931 8791
www.metoffice.com

*Designed and produced by the Met Office © Crown copyright 2001 01/0240 The Met Office logo is a registered trademark.*

# PARAMETRIZATION OF DIABATIC PROCESSES IN THE INVERSION OF THE OMEGA-EQUATION

by

Athanassiadou M.* and A. J. Thorpe

Joint Centre for Mesoscale Meteorology,

UK Meteorological Office / University of Reading, UK

June 1996

## *ABSTRACT*

This Technical Report introduces an improvement to the parametrization of diabatic processes in the inversion of the quasi-geostaophic omega-equation.

It was found that the currently used algorithm sometimes produces predictions of vertical velocities due to diabatic processes which are in excess, in places, of the total model vertical velocities. This is due to the fact that the omega-equation does not always remain elliptic with the currently used algorithm. Corrective action is taken by setting the moist static stability parameter, $\sigma_m$, a small fraction of the dry static stability, $\sigma$, when the former becomes negative i.e., $\sigma_m = C\,\sigma$ ($C$ is a constant) when $\sigma_m < 0$.

The new algorithm was tested for a range of different values of the constant $C$, from $C$=0.1 to $C$=0.01. The results show that the choice of the constant C does not significantly affect the retrieved vertical velocities. On the other hand, such corrective action is necessary in order to obtain realistic vertical velocities due to diabatic processes from the inversion of the omega-equation.

*Corresponding Author address: Dept. of Meteorology, University of Reading, 2 Earley Gate, Whiteknights, PO Box 239, Reading, Berkshire RG6 6AU, UK.

## 1. INTRODUCTION

The quasi-geostrophic (QG) omega-equation is a useful tool to investigate processes affecting synoptic-scale vertical motions. From the different forms of the QG omega-equation that have been developed the Q-vector form is the most "compact" since in this formulation, the vertical velocity is forced solely by the divergence of $\bar{Q}$, (Hoskins et al. 1978, Clough et al. 1995).

Numerical inversion of the QG omega-equation with appropriate boundary conditions enables us to quantify the contributions from the different mechanisms (synoptic, diabatic etc.) to the total vertical motion, so that the relative importance of the different processes can be evaluated. Case studies have shown the importance of diabatic heating in the enhancement of vertical motions, (e.g. Krishnamurti 1968b, Clough and Davitt 1994, Athanassiadou and Thorpe 1995).

Here, the contribution of diabatic processes to the total vertical motion is re-examined. The QG omega-equation is solved using data from the Unified Model at a horizontal resolution of ~ 100 *Km*, and a vertical resolution of 100 *mb* from 1000 *mb* to 100 *mb*.

In section 2, the Q-vector form of the omega-equation and the method of solution is highlighted. In section 3 the current formulation of the algorithm that treats diabatic forcing is presented. The new improved code is also given in section 3. Sensitivity tests and comparisons are given in section 4. In section 5, an overview of the results and a discussion is presented.

## 2. THE OMEGA-EQUATION AND METHOD OF SOLUTION

The Q-vector form of the QG ω-equation in pressure coordinates, with diabatic and frictional effects included is given by:

$$\nabla_p^2\,\sigma(p)\omega + f_o^2\frac{\partial^2\omega}{\partial p^2} = -2\nabla_p\cdot\bar{Q} - \frac{R}{p}\nabla_p^2\left(\frac{\dot{q}}{c_p}\right) - f_o\bar{k}\cdot\left(\nabla_p\times\frac{\partial F}{\partial p}\right) \qquad (1)$$

where,

$$\bar{Q} = -\frac{R}{p}\left(\frac{p}{p_o}\right)^k \begin{pmatrix} \frac{\partial \bar{v}_g}{\partial x}\cdot\nabla q \\ \frac{\partial \bar{v}_g}{\partial y}\cdot\nabla q \end{pmatrix} \quad ; \quad \sigma(p) = -\frac{R\bar{T}(p)}{p}\frac{\partial \ln \bar{q}(p)}{\partial p} \qquad (2)$$

$F$ stands for friction in general and $\dot{q}$ is the diabatic heating rate.

Equation (1) is solved in the "free"-atmosphere. In this case friction on the rhs of (1) is taken $F = 0$. Terrain and frictional effects are nevertheless enter through the lower boundary conditions. In general, frictional effects can be significant not only near the ground but at upper levels as well, near strong jets and in regions of deep cumulus convection.

The operator $\mathcal{L} = \nabla_h^2 + (f_o^2/\sigma)(\partial^2/\partial p^2)$ in (1) is linear since $\sigma$ and $f_o^2$ are not functions of $\omega$ or derivatives of $\omega$. In the quasi-geostrophic theory $\sigma$ must only depend on $p$. Currently $\sigma$ is evaluated as a horizontal average of the local values of static stability. Furthermore, equation (1) is elliptic provided that $-4(f_o^2/\sigma) < 0$ that is, when $\sigma > 0$ (statically stable atmosphere).

The problem of the QG $\omega$-equation inversion consists of the solution of a linear PDE equation with appropriate boundary conditions. The schematic diagram in Fig. 1 summarises the procedure. In its general form, this problem is non-homogeneous in two ways; due to the forcing function $\mathcal{D}$ on the rhs of (1) and the boundary conditions $\mathcal{A}$. The vertical velocity $\omega$ can be decomposed into two parts, $\omega = \omega_1 + \omega_2$, one $\omega_1$ due to the forcing $\mathcal{D}$ and the other $\omega_2$ due to the boundary condition. It is easily checked that $\omega = \omega_1 + \omega_2$ satisfies the original equation and the non-homogeneous BC.

The solution for $\omega_2$ can be further decomposed into $\omega_2 = \omega_{2sb} + \omega_{2mt}$, one $\omega_{2sb}$ due to the lateral BC and a $\omega_{2mt}$ due to the lower BC. Furthermore, the solution for $\omega_1$ can be further decomposed into $\omega_1 = \omega_{1so} + \omega_{1dh}$, one $\omega_{1so}$ due to the synoptic scale only (dynamic) forcing and a $\omega_{1dh}$ due to diabatic heating. The forcing function of the later is associated with all processes except for dry adiabatic ascent and descent. In general, it contains two components of heating: (a) that due to diabatic processes such as radiation, turbulent mixing, surface sensible heating and cumulus convection ($\mathcal{D}_{ND}$), nor resolved by the model data; and (b) that resulting from resolved moist adiabatic ascent ($\mathcal{D}_{MA}$).

The partitioning described thus far has the feature that

$$\omega = \omega_{1so} + \omega_{1dh} + \omega_{1sb} + \omega_{2mt} = \omega_{1so} + \omega_{1nd} + \omega_{1ma} + \omega_{2sb} + \omega_{2mt} \qquad (3)$$

so that the total vertical velocity ω can be decomposed into different parts, each being the contribution to the vertical motion from different, interrelated nevertheless, mechanisms. The above decomposition is not the only one possible, but it is the one that gives more insight into the role of individual processes.

## *2.1 Diabatic forcing (latent heat release)*

In general, $\dot{q} = \dot{q}_{ma} + \dot{q}_{nd}$ ; where $\dot{q}_{ma}$ is due to moist ascent and $\dot{q}_{nd}$ is due to all forms of heating (or cooling) not resulting from dry or moist adiabatic ascent or descent in synoptic-scale systems.

The ω component associated with diabatic heating will be assumed only associated with diabatic heating from latent-heat release in regions of precipitation $\dot{q}_{ma}$. This is considered the dominant process for synoptic-scale vertical motions. Indeed, in limited areas of heavy precipitation, condensation heating can easily surpass 1 *K/h* in deep layers (assuming a precipitation rate of 4 *mm/h*), whereas radiative cooling, for example, seldom exceeds a few degrees per day. Typically, strong condensation heating induces a core of intense rising motion and a wider surrounding belt of weak subsidence.

The ω component that is associated with latent heat release is the solution to

$$\nabla_p^{\,2}\,\sigma(p)\omega_{ma} + f_o^2\frac{\partial^2\omega_{ma}}{\partial p^2} = -\frac{R}{p}\nabla_p^{\,2}\left(\frac{\dot{q}_{ma}}{c_p}\right) \quad ; \quad \omega_{ma} = 0 \quad \text{(BC)} \qquad (4)$$

Therefore $\omega_{ma}$ represents the *"enhancement"* in the vertical motion due to the fact that ascent takes place on a saturated environment.

To find the contribution to the vertical motion from diabatic heating it is necessary to evaluate $\dot{q}_{ma}$. Generally this is not an observed quantity so that it must be diagnostically calculated. It is often the case (for ascent following a moist adiabat) that $\dot{q}_{ma}$ can be related to the vertical motion itself. So we can express the diabatic heating rate per unit mass associated with moist ascent as:

$$\dot{q}_{ma} = \begin{cases} -L\dfrac{\partial q_s}{\partial p}\omega, & \text{when the air is saturated and rising} \\ 0 & \text{otherwise} \end{cases} \qquad (5)$$

A better alternative is to find $\dot{q}$ used in the model initialisation or forecast. As this is not available routinely, equation (5) is a practical and straightforward way to estimate $\dot{q}$.

Equation (4) is therefore written as

$$\nabla_p^{\,2}\,\sigma(p)\omega_{ma} + f_o^2\frac{\partial^2\omega_{ma}}{\partial p^2} = \frac{RL}{c_p\,p}\nabla_p^{\,2}\left[\frac{1}{2}(\omega - |\omega|)\frac{\partial q_s}{\partial p}\right] \qquad (6)$$

A static stability parameter for moist air can be given in terms of the equivalent potential temperature as:

$$\sigma_m(p) = -\frac{R\overline{T}(p)}{p}\frac{\partial \ln\overline{\theta}_e(p)}{\partial p} \quad ; \quad \overline{\theta}_e = \overline{\theta}\exp(Lq_s/c_p\overline{T}) \qquad (7)$$

Moreover, the relation between $\sigma$ and $\sigma_m$ can be obtained from (2) and (7):

$$\sigma_m = \sigma - \frac{\delta RL}{c_p\,p}\frac{\partial q_s}{\partial p} \quad ; \quad \delta = \begin{cases} 1, & \text{for } q = q_s \ \wedge \ \omega < 0 \\ 0 & \text{for } q < q_s \ \vee \ \omega > 0 \end{cases} \qquad (8)$$

and (6) can be written as:

$$\nabla_p^{\,2}\,\sigma_m(p)\omega_{ma} + f_o^2\frac{\partial^2\omega_{ma}}{\partial p^2} = \frac{RL}{c_p\,p}\nabla_p^{\,2}\left[\frac{1}{2}(\omega_R - |\omega_R|)\frac{\partial q_s}{\partial p}\right] \qquad (9)$$

where $\omega_R = \omega - \omega_{ma}$ is the (synoptic-scale) part of vertical motion due to all processes apart from the latent heat release. Equation (9) remains elliptic as long as $\sigma_m > 0$. Note that although $\sigma$ is only a function of $p$, the quantity $\sigma_m$ can and does also vary in the horizontal.

Equations (6) and (9) are alternative forms giving the same contribution $\omega_{1ma}$. It is clear that the interpretation of $\omega_{1ma}$ is that it is the *additional* vertical motion that exists because the atmosphere locally is saturated and releases latent heat. It represents an amplification of that part of the vertical motion which exists due to synoptic-scale forcing in a dry atmosphere.

Note that the inherent significance of this additional contribution $\omega_{1ma}$ is not diminished by using the model total $\omega$ to evaluate $\dot{q}$.

## 3. THE NEW IMPROVED CODE

### 3.1 Current method of solution

The inversion of the omega-equation is among the diagnostics available from the Unified Model. This is done with the MDIAG - set of programmes. Current settings include zero vertical velocity at all boundaries.

Diabatic processes are parametrized in a manner analogous to the one described in Section 2. In particular, the vertical velocity associated with latent heat release is obtained from:

$$\nabla_h^2\,\sigma(p)\omega_{1ma} + f_o^2\frac{\partial^2\omega_{1ma}}{\partial p^2} = \frac{RL}{c_p p}\nabla^2\left(\omega_{MODEL}\,\frac{\partial q_s}{\partial p}\right)\quad;\quad \omega_{1ma}=0 \quad \text{(BC)} \qquad (10)$$

following the procedure described below.

The $\omega$ in the forcing term is taken from the model output. Generally $\omega_{MODEL} \neq \omega$ and in that respect, the diabatic forcing term somewhat differs from the approach in section 2. This is because $\omega_{MODEL}$ embodies vertical motion due to all possible physical processes, even those not included in the quasi-geostrophic omega equation. Different values of $L$ are assumed depending on whether the temperature is above or below zero. Moreover, both negative and positive values of $\omega$ enter the rhs of (10) and the diabatic forcing is zero, only when the RH with respect to ice is less than 85%.

### 3.2 Suggested method of solution

Proper solution of the omega-equation requires that (10) remains always elliptic. In turn, this requirement is satisfied when the effective static stability $\sigma_m = \sigma - \frac{RL}{c_p p}\frac{\partial q_s}{\partial p}$ is always positive. This condition though, is not satisfied everywhere. The unrealistic vertical velocities due to diabatic forcing which are obtained from the inversion of the omega-equation are believed to exist because of the violation of the requirement $\sigma_m > 0$.

When $\sigma_m < 0$ but $\sigma > 0$, the atmosphere is conditionally unstable and the parametrization of the diabatic processes needs a different formulation (Krishnamurti 1968a). In the improved scheme, proposed here, an adjustment is made to the effective static stability $\sigma_m$ when this becomes negative. The adjustment consists of setting the effective static stability equal to a small number times the static stability when the former is negative.

$$\sigma_m < 0 \quad \Rightarrow \quad \sigma_m = C\,\sigma \quad ; \quad C = const. \tag{11}$$

This is equivalent to the neglect of conditionally unstable regions. The choice of a reasonable value for $C$ is not obvious, apart from the fact that it should be a small number. Different values of $C$ where considered in the range 0.1 to 0.01. The new scheme was tested for the case studies of the ANOMALIA project (Athanassiadou and Thorpe, 1996). Results from one of the case studies, using the new scheme, are presented in the next section.

## 4. RESULTS

Model vertical velocities as well as vertical velocities obtained from the inversion of the omega-equation with both the old and the new scheme are shown for the 12Z of the 23/9/93 on the 700 *mb*. The experiments using the new scheme are summarised in Table 1.

Fig. 2 shows the vertical velocity $w_{MODEL}$, the model output. Solid and dotted contour lines in this figure, as well as subsequent ones, encompass vertical velocities $\geq 2\ cm\ s^{-1}$ and $\leq -2\ cm\ s^{-1}$ respectively. Two points, A and B, are chosen to facilitate the inter comparison of the results. Point A is over the Atlantic ($x$=2438.4 $y$=812.8), in the area of maximum ascent.

Point B is over the western Mediterranean ($x$=5791.2, $y$=914.4). The results are summarised in Table 2.

| Experiment | name | $\sigma_m = C\,\sigma$ | Diabatic forcing ≠ 0 when RH > 85% and |
|---|---|---|---|
| 1 | ns | $C$=0.1 | $\omega < 0$ only |
| 2 | nl | $C$=0.01 | $\omega < 0$ only |
| 3 | si | $C$=0.01 | $\omega < 0$ and $\omega > 0$ |

**Table 1:** Summary of the settings for the experiments performed with the new scheme.

| Point | A | B |
|---|---|---|
| $w_{MODEL}$ *cm/s* | 16.6 | 14.1 |
| $w$ (old scheme) *cm/s* | 22.8 | 17.4 |
| $w$ (ns) *cm/s* | 13.1 | 10.6 |
| $w$ (nl) *cm/s* | 14.4 | 11.6 |
| $w$ (si) *cm/s* | 14.5 | 11.6 |
| $w$ (synoptic forcing) *cm/s* | ~0.0 | 1.4 |

**Table 2:** Vertical velocities for points A and B, from the model and the inversion of the omega equation using the different schemes. Also given is the calculated vertical velocity from the synoptic forcing.

The vertical velocity calculated from the inversion of the omega-equation using the old scheme is shown in Fig. 3. This, as well subsequent figures show just the diabatic contribution. Although the overall pattern seems quite reasonable, closer inspection of the maximum values of $w$, in Fig. 3, reveals that, in places, these are in excess of the $w_{MODEL}$. In particular, the vertical velocity using the old scheme is 37% in excess of $w_{MODEL}$ at point A and 24% at point B. This does not seem a very realistic solution.

In the first of the experiments performed with the improved scheme (ns), the effective static stability was set equal to 0.1 times the static stability when the former became negative. The vertical velocity from the inversion of the omega-equation for the experiment ns, is shown in Fig. 4.

With the new algorithm, the vertical velocity due to diabatic processes $w_{ma}$, is realistic. Nowhere in the domain $w_{ma}$ exceed $w_{MODEL}$. In particular, $w_{ma}$ at points A and B are 79% and 75% of $w_{MODEL}$ at the same points respectively. Clearly this is an improvement to the existing algorithm toward realistic vertical velocities due to diabatic forcing.

The sensitivity of the solution to the choice of the constant $C$ used in the new formulation was examined for a variety of different values of $C$. Fig. 5 shows the results from the second experiment (nl) in which $C$=0.01, an order of magnitude smaller than it was in the first experiment (ns). The overall pattern of $w_{ma}$ in Fig. 5 is almost identical to the one in Fig. 4 (experiment ns). Slightly larger values are obtained in this case at points A and B compared with the values obtained at the same points in the experiment ns. In particular, $w_{ma}$ at A is now 87% and at B 82% of $w_{MODEL}$. This amounts to a difference of the order of 7-8% between the two cases.

Finally, one further test was performed in order to assess whether the diabatic forcing should be evaluated for rising air only or for both rising and descending motion. This latter case might be relevant if evaporation of precipitation is effective. As the diabatic forcing is only used on descent for RH $\geq$ 85%, then this may be a realistic representation. The results from this third experiment (si), are shown in Fig. 6. The constant C in this case is C=0.01 so that comparisons should really be made with Fig. 5 (experiment nl) and Fig. 2 (the model vertical velocity).

The overall pattern of ascending $w_{ma}$ virtually identical to the one of the experiment nl. This is also true for the maximum values of the obtained updrafts, Table 2. The only difference between the experiments nl and si is in the obtained downdrafts. This is particularly the case in the western Mediterranean region, behind the strong frontal system in the area (not shown but somewhat obvious from the vertical velocity pattern in Fig. 2).

## 5. DISCUSSION

It is clear from the results presented in the previous section that the existing code needs to be adjusted if reasonable vertical velocities due to diabatic forcing are to be obtained from the inversion of the QG omega-equation. With the currently employed algorithm, the omega-equation does not remain elliptic throughout the domain where solution is sought.

The simple solution to the problem, suggested in this report has shown that reasonable results can be obtained by setting the effective static stability equal to a small constant times the static stability, when the former becomes negative. Under this approach, conditionally unstable regions are neglected. A more advanced improvement, and probably a better one, would be to parametrize appropriately, moist processes under unstable conditions. This is left as future research.

Finally, it seems better to apply the parametrization to both rising and descending motion as long as the diabatic forcing is only evaluated for nearly saturated air. The main difference between this and restricting diabatic forcing to rising motion is in the downdrafts, especially behind strong frontal systems, calculated from the inversion of the omega-equation.

## 6. ACKNOWLEDGEMENTS

This work is supported by the EC contract EV5V-CT94-0442.

We would like to thank Sid Clough for helpful discussions.

## *REFERENCES*

Athanassiadou M., and A. J. Thorpe 1995: "The ANOMALIA project and MAP", *MAP Newsletter*, **No. 3**, 48 - 50.

Athanassiadou M., and A. J. Thorpe 1996: "Omega-equation attribution applied to severe weather events in the Western Mediterranean", *Proceedings of 7th Conference on Mesoscale Processes,* Reading 9-13 September.

Clough S. A. and Clare S. A. Davitt, 1994: "Development of an Atlantic frontal wave during IOP 3 of fronts '92" in The Life Cycles of Extratropical Cyclones, **II**, 151-156, *International Symposium 27/6-1/7 94*, Bergen, Norway.

Clough S. A., C. S. A. Davitt and A. J. Thorpe, 1995: "Attribution concepts applied to the omega equation", *JCMM Internal Report 47.*

Hoskins B. J., I. Draghici and H. C. Davies, 1978: "A new look at the omega-equation". *Quart. J. R. Meteor. Soc.*, **104**, 31-38.

Räisänen J., 1995: "Factors affecting synoptic-scale vertical motions: A statistical study using a generalised omega equation", *Mon. Wea. Rev.*, **Vol. 123**, 2447-2460

Ray P. S., 1986 (ed): Mesoscale meteorology and forecasting, *AMS*, pp 793

Krishnamurti T. N., 1968a: "A diagnostic balance model for studies of weather systems of low and high latitudes, Rossby number less than 1", *Mon. Wea. Rev.*, **Vol. 96, No 4**, 197-207

Krishnamurti T. N., 1968b: "A study of a developing wave cyclone", *Mon. Wea. Rev.*, **Vol. 96, No 4**, 208-217

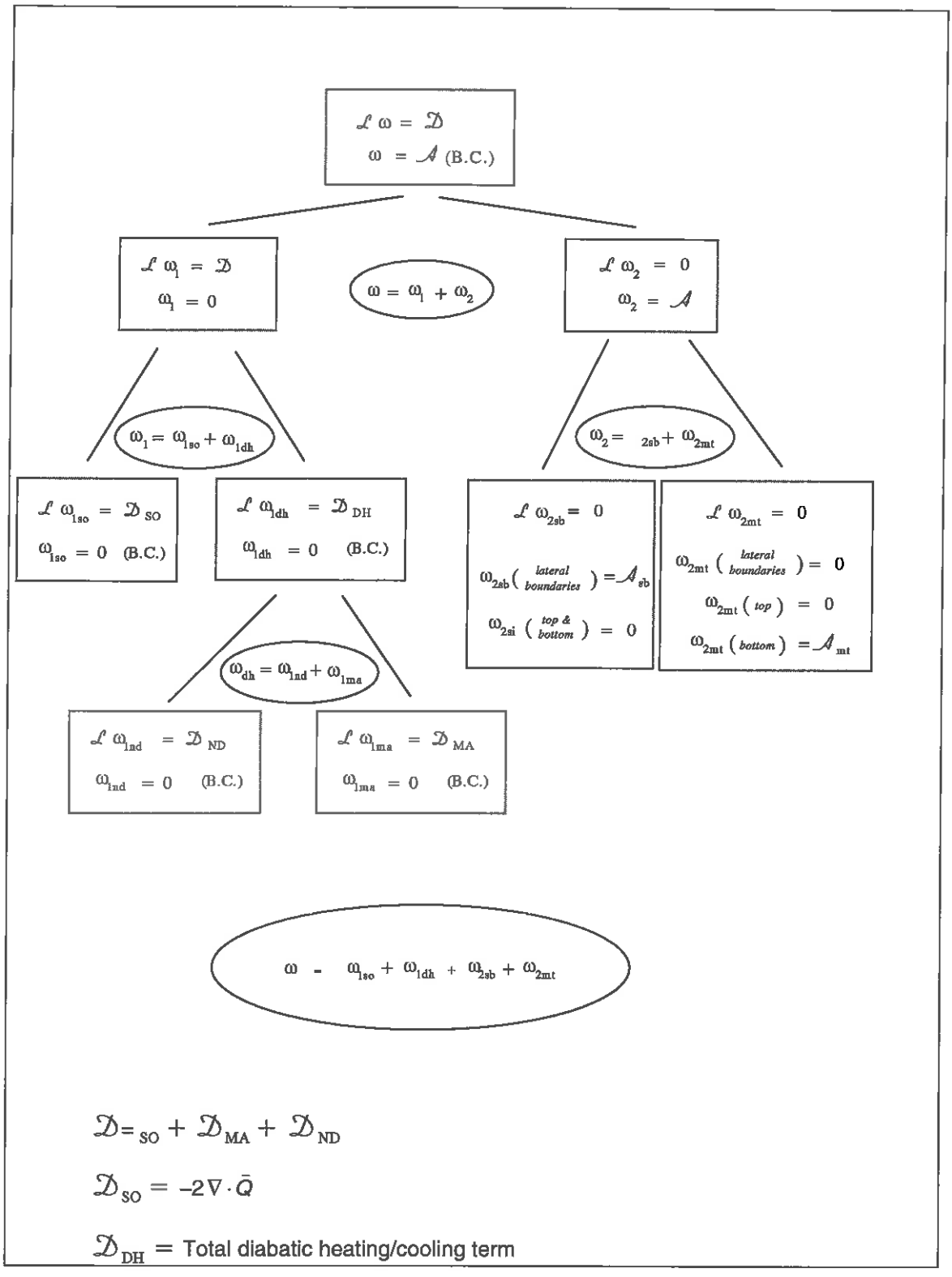


***Figure 1:*** Schematic diagram of the solution of the omega-equation in general

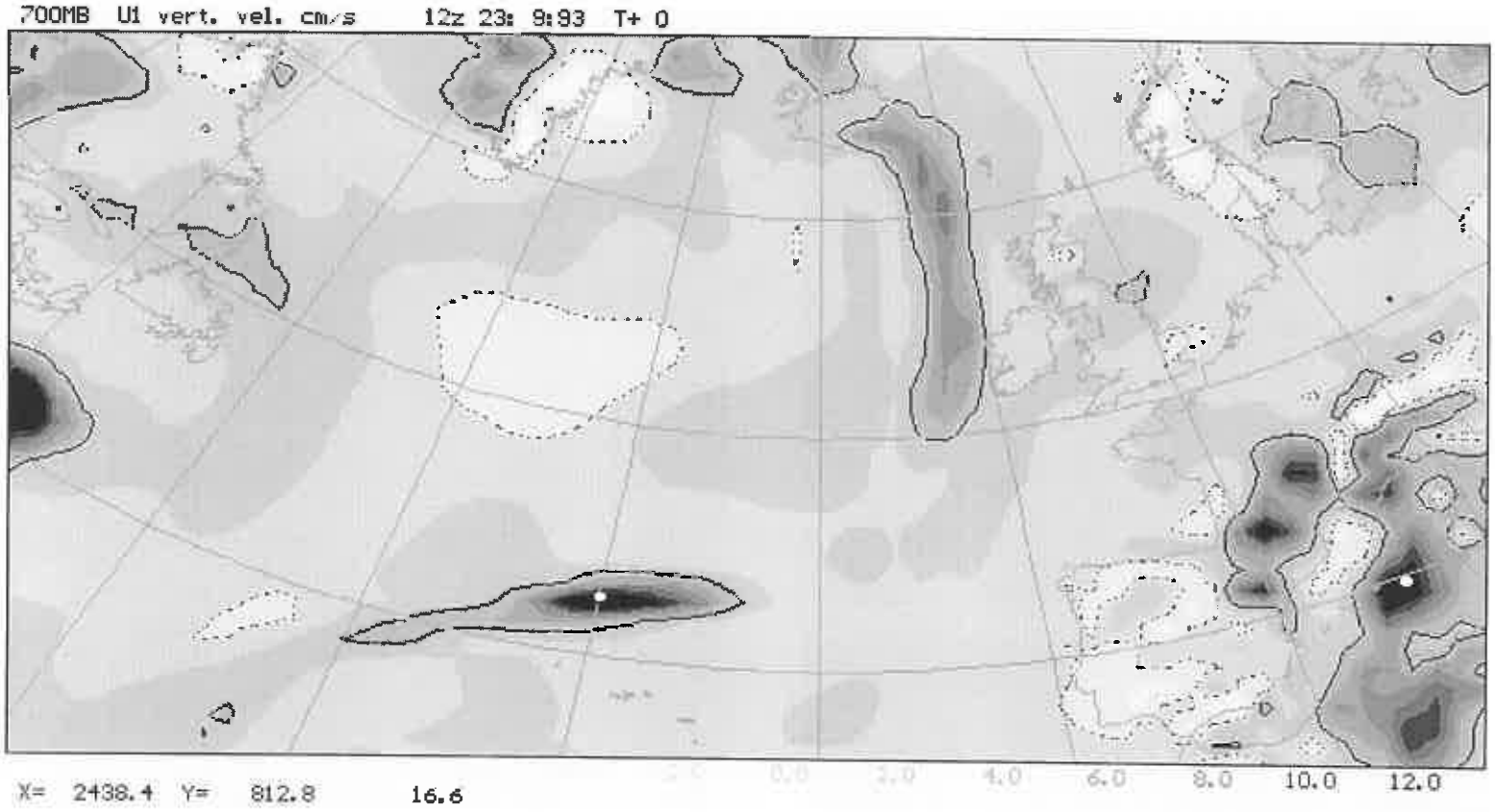


MODEL VERTICAL VELOCITY

**Figure 2:** Vertical velocity. Contours: Solid 2 cm/s. Dotted -2 cm/s

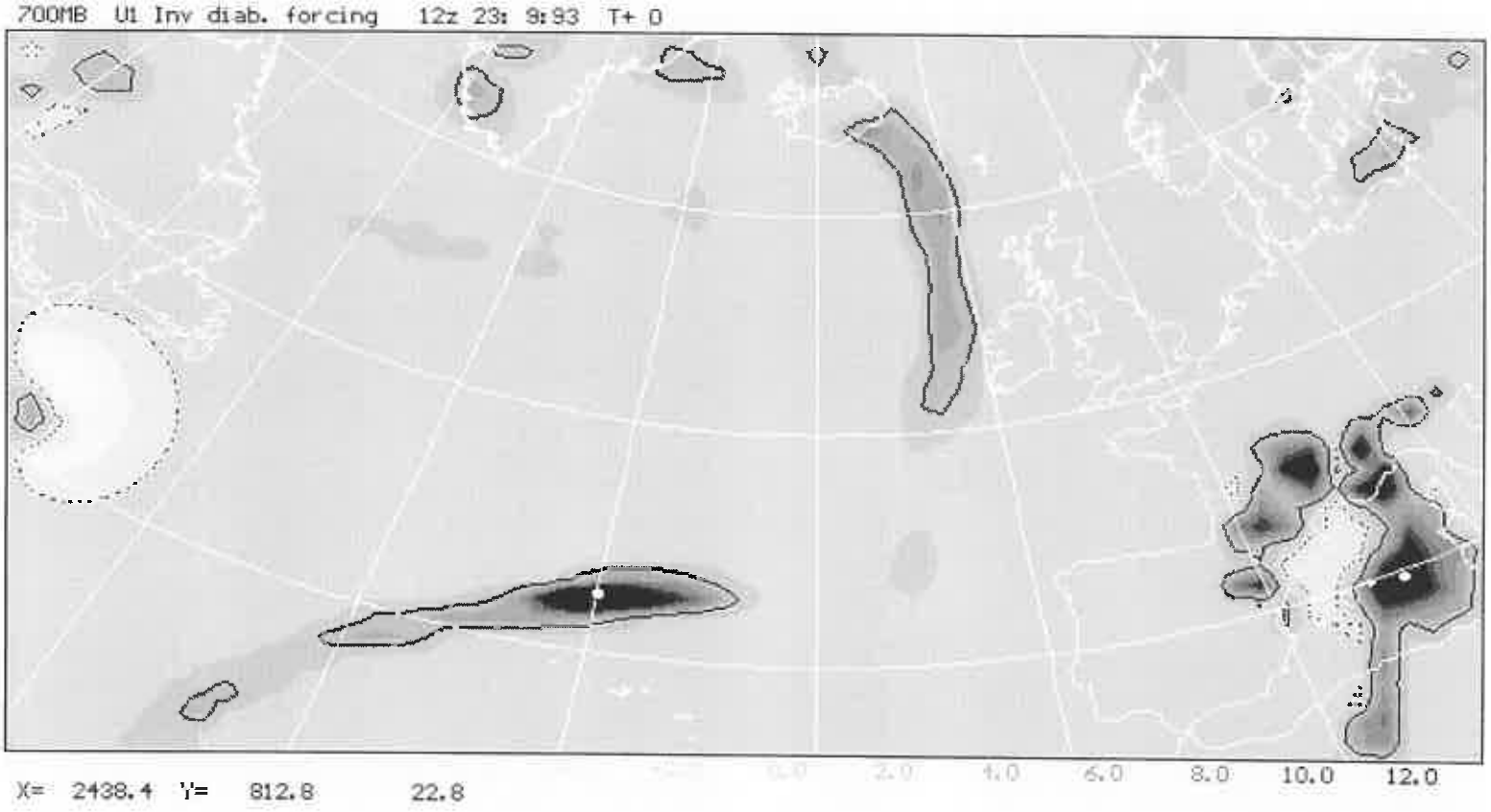


OLD SCHEME

**Figure 3:** Vertical velocity. Contours: Solid 2 cm/s. Dotted -2 cm/s

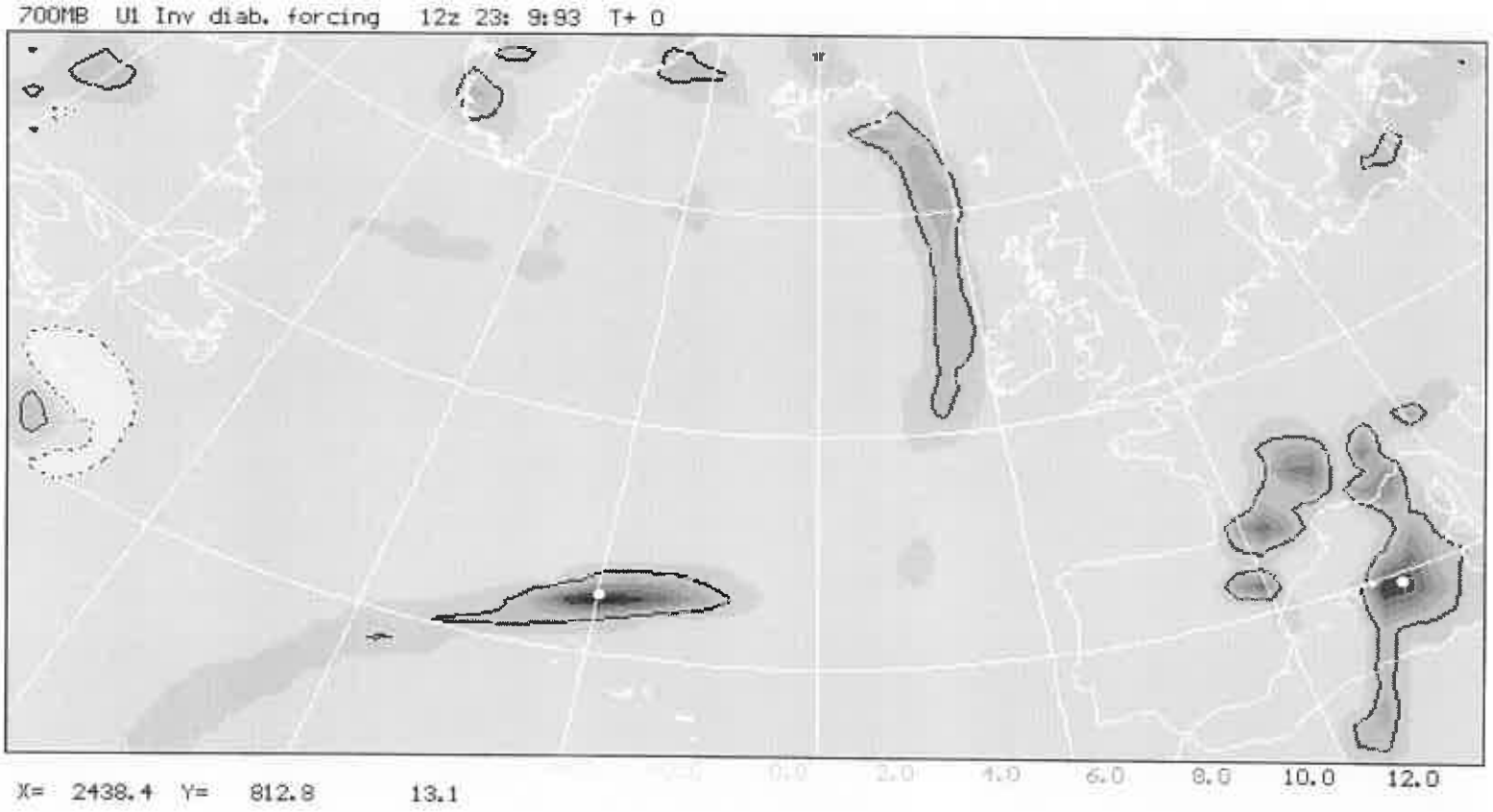


EXPERIMENT 1 (ns)

**Figure 4:** Vertical velocity. Contours: Solid 2 cm/s. Dotted -2 cm/s

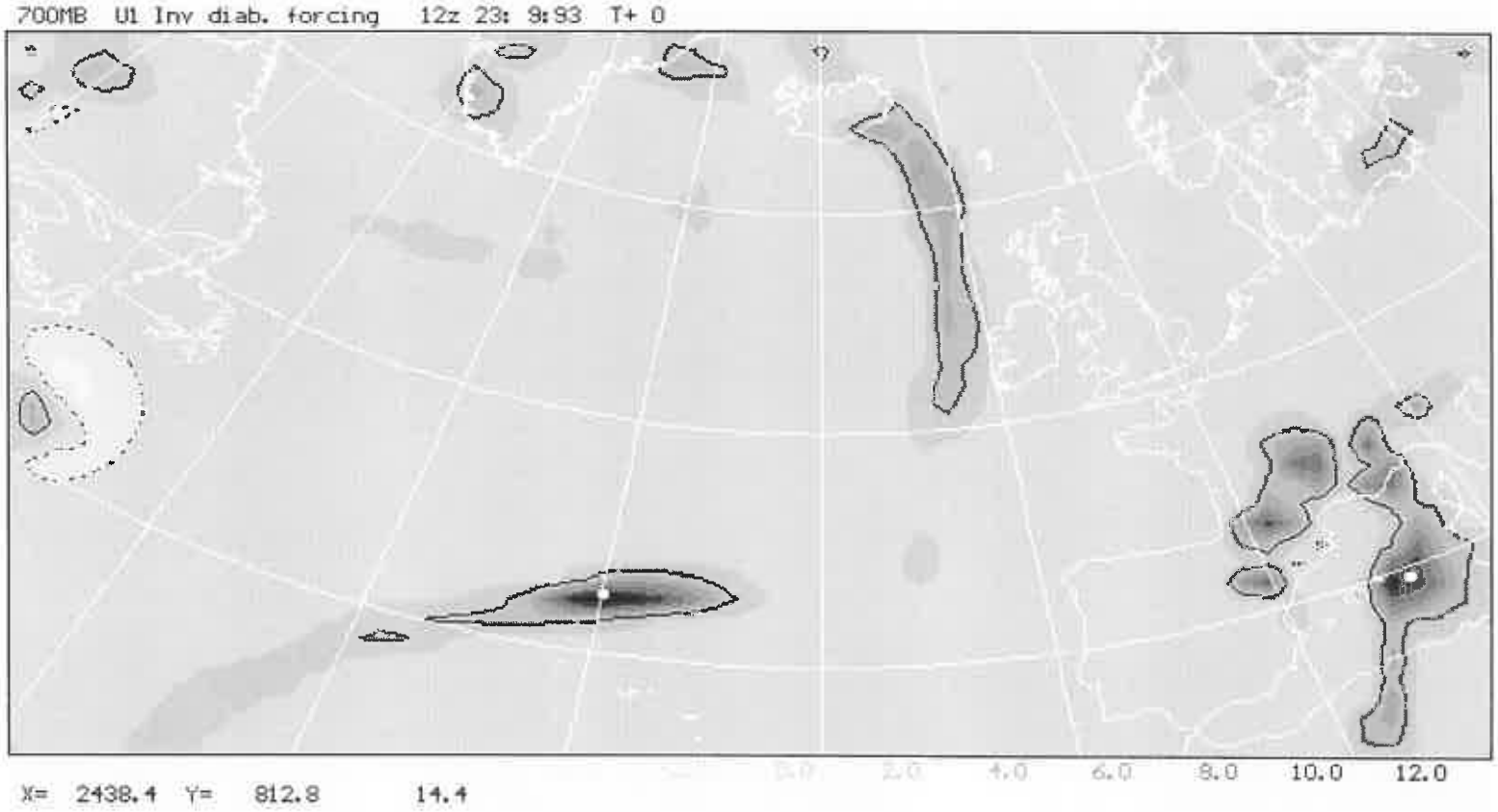


EXPERIMENT 2 (nl)

**Figure 5:** Vertical velocity. Contours: Solid 2 cm/s. Dotted -2 cm/s

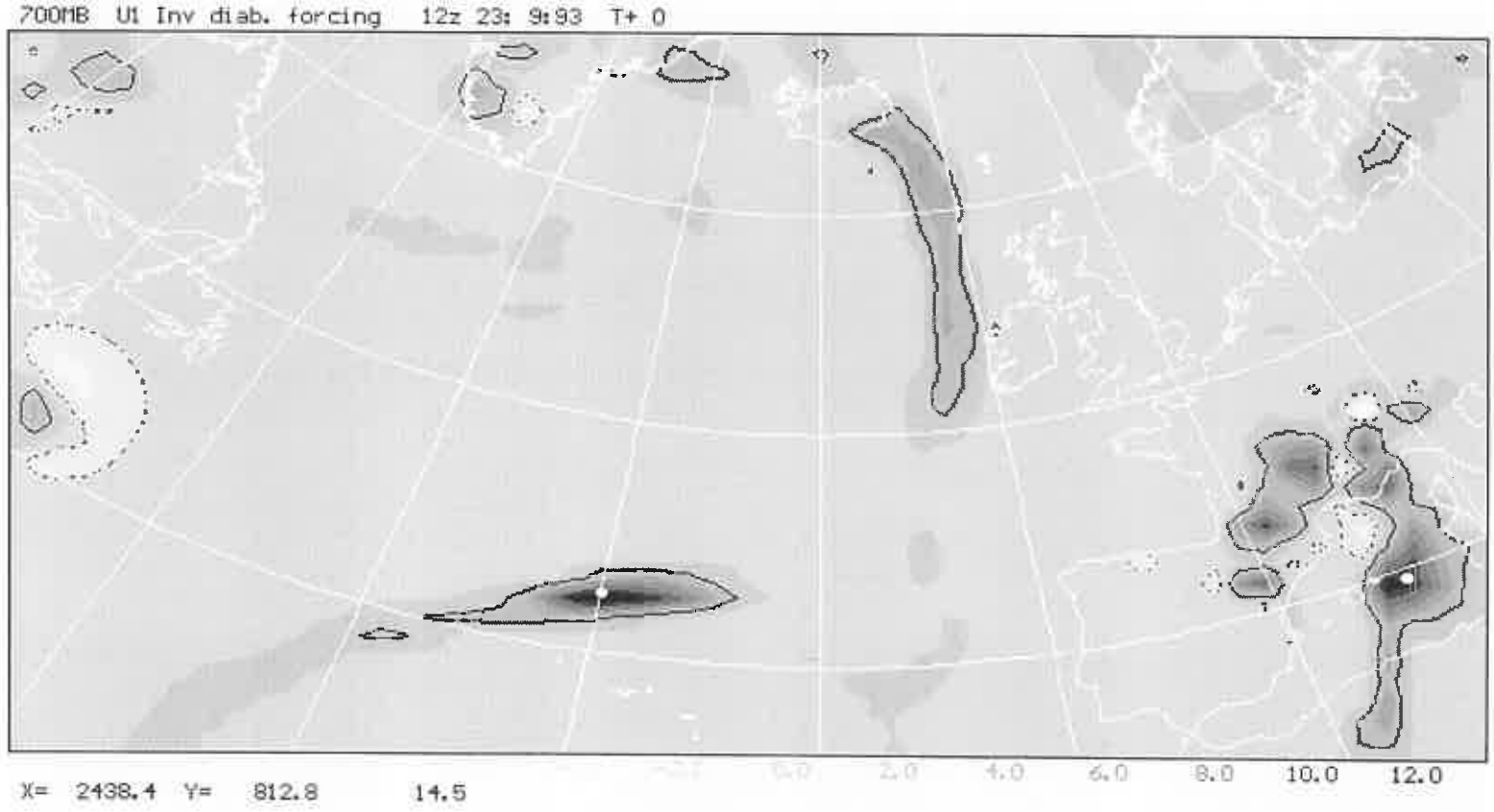


EXPERIMENT 3 (si)

**Figure 6:** Vertical velocity. Contours: Solid 2 cm/s. Dotted -2 cm/s

## *CURRENT JCMM INTERNAL REPORTS*

1. **Research Strategy and Programme**
   K. A. Browning et al.
   Jannuary 1993

2. **The GEWEX Cloud System Study (GCSS)**
   GEWEX Cloud System Science Team
   Jannuary 1993

3. **Evolution of a mesoscale upper tropospheric vorticity maximum and comma cloud from a cloud-free two-dimensional potential vorticity anomaly.**
   K. A. Browning
   Jannuary 1993

4. **The global Energy and Water Cycle**
   K. A. Browning
   July 1993

5. **Structure of a Midlatitude Cyclone before Occlusion**
   K. A. Browning and N. Roberts
   July 1993

6. **Developments in Systems and Tools for Weather Forecasting**
   K. A. Browning and G. Szejwach
   July 1993

7. **Diagnostic Study of a Narrow Cold Frontal Rainband and Severe Winds Associated with a Stratospheric Intrusion**
   K. A. Browning and R. Reynolds
   August 1993

8. **Survey of Perceived Priority issues in the Parametrizations of Cloud-related processes in GCMs**
   K. A. Browning
   September 1993

9. **The Effect of Rain on Longwave Radiation**
I. Dharssi
September 1993

10. **Cloud Microphysicla Processes - A Description of the Parametrization used in the Large Eddy Model**
H. Swann
July 1994

11. **An Appreciation of the Meteorological Research of Ernst Kleinschmidt**
A. J. Thorpe
May 1992

12. **Potential Vorticity of Flow along the Alps**
A. J. Thorpe, H. Volkert and D. Heimann
August 1992

13. **The Representation of Fronts**
A. J. Thorpe
January 1993

14. **A Parametrization Scheme for Symmetric Instability: Tests for an Idealised Flow**
C. S. Chan and A. J. Thorpe
February 1993

15. **The Fronts 92 Experiment: A Quicklook Atlas**
Edited by T. D. Hewson
November 1993

16. **Frontal Wave Stability during Moist Deformation Frontogenesis.**
**Part 1. Linear Wave Dynamics**
C. H. Bishop and A. J. Thorpe
May 1993

17. **Frontal Wave Stability during Moist Deformation Frontogenesis.**
**Part 2. The Suppression of Non-Linear Wave Development**
C. H. Bishop and A. J. Thorpe

May 1993

18. **Gravity Waves in Sheared Ducts**
S. Monserrat and A. J. Thorpe
October 1993

19. **Potential vorticity and the Electrostatics Analogy: Quasi-Geostrophic Theory**
C. H. Bishop and A. J. Thorpe
November 1993

20. **Recent Advances in the Measurement of Precipitation by Radar**
A. J. Illingworth
April 1993

21. **Micro-Physique et Givrage. Cloud Microphysics and Aircraft Icing**
A. J. Illingworth
May 1993

22. **Differential Phase Measurements of Precipitation**
M. Blackman and A. J. Illingworth
May 1993

23. **Estimation of Effective Radius of Cloud Particles from the Radar Reflectivity**
N. I Fox and A. J. Illingworth
May 1993

24. **A Simple Method of Dopplerising a Pulsed Magnetron Radar**
L. Hua, A. J. Illingworth and J. Eastment
November 1993

25. **Radiation and Polar Lows**
George C Craig
February 1994

26. **Collected preprints submitted to International Symposium on the Life Cycles of Extratropical Cyclones; Bergen, Norway, 27 June - 1 July 1994**
April 1994

27. **Convective Frontogenesis**
Douglas J Parker and Alan J Thorpe
April 1994

28. **Improved Measurement Of The Ice Water Content In Cirrus Using A Total Water Evaporator**
Philip R A Brown and Peter N Francis
April 1994

29. **Mesoscale Effects of a Dry Intrusion within a Vigorous Cyclone**
K A Browning and B W Golding
April 1994

30. **GEWEX Cloud System Study, Science Plan**
May 1994

31. **Parametrization of Momentum Transport by Convectively Generated Gravity Waves**
R Kershaw
May 1994

32. **Mesoscale Modelling Newsletter, No. 5**
May 1994

33. **Observations of the mesoscale sub-structure in the cold air of a developing frontal cyclone**
K A Browning, S A Clough, C S A Davitt, N M Roberts and T D Hewson
May 1994

34. **Longwave Radiative Forcing of a Simulated Tropical Squall Line**
Imtiaz Dharssi
July 1994

35. **On the nature of the convective circulations at a kata-cold front**
K A Browning
September 1994

36. **Collected preprints of papers submitted to the COST-75 International Seminar on Advanced Weather Radar Systems, Brussels, 20-23 September 1994**
November 1994

37. **Use of Satellite imagery to diagnose events leading to frontal thunderstorms: Parts I and II of a case study**
K A Browning and N M Roberts
November 1994

38. **The role of a spaceborne millimetre-wave radar in the global monitoring of ice cloud**
P R A Brown, A J Illingworth, A J Heymsfield, G M McFarquhar, K A browning
December 1994

39. **Potential Vorticity Inversion**
Michal Ziemianski
October 1994

40. **Theory of mature tropical cyclones; A compariosn between Kleinschmidt (1951) and Emanual (1986)**
Suzanne L Gray
December 1994

41. **Dispersion and removal of pollutants during the passage of an atmospheric frontal system**
N R Gimson
December 1994

42. **The role of snow sublimation in frontogenesis**
D J Parker and A J Thorpe
December 1994

43. **Potential vorticity and the electrostatics Analogy: Ertel-Rossby formulation**
A J Thorpe and C H Bishop
December 1994

44. **Mesoscale aspects of extratropical cyclones: an observational prespective**
K A Browning
January 1995

45. **A Polar Low Outbreak: Evolution and Mesoscale Structures**
T D Hewson, G C Craig and C Claud
February 1995

46. **Generation of Near-Surface Gusts by Deep Convection**
K. Nakamura and R. Kershaw
April 1995

47. **Attribution Concepts Applied to the Omega Equation**
S. A. Clough, C. S. A. Davitt and A. J. Thorpe
June 1995

48. **Parametrization of mixed-phase cloud and precipitation**
Susan P. Ballard, and M. Gerard Hutchinson
June 1995

49. **Short-range forecasting of stratocumulus: Initialization V prediction**
Susan P. Ballard, Simon D. Jackson and B. Macpherson
June 1995

50. **Contributions of the JCMM/Dept of Meteorology Radar Group to the 27th AMS Radar Meteorology Conference, Vail October 1995**
June 1995

51. **Could pools in shear**
Douglas J. Parker
September 1995

52. **High-resolution analysis of frontal fracture**
K. A. Browning, S. P. Ballard, and C. S. A. Davitt
September 1995

53. **The Albedo of Broken Cloud Fields: Calculations using a modified two stream radiation code**
Imtiaz Dharssi and Roy Kershaw
October 1995

54. **Parametrization of momentum transport by convection. I: Theory and cloud modelling results**
Roy Kershaw and D. Gregory
November 1995

55. **Variation of frontal structure along a cold front**
K. A. Browning and N. M. Roberts
November 1995

56. **Secondary frontal waves**
Douglas J. Parker
December 1995

57. **Objective Fronts**
T. D. Hewson
March 1996

58. **Mesoscale analysis of the activation of a cold front during cyclogenesis**
K. A. Browning, N. M. Roberts and A. J. Illingworth
June 1996

59. **Investigation of different presentations of rain in a 1-d evaporation model**
H. Swann
May 1996

60. **Parametrization of diabatic processes in the inversion of the omega-equation**
Maria Athanassiadou and Alan J. Thorpe
June 1996

**Met Office** Joint Centre for Mesoscale Meteorology Department of Meteorology
University of Reading PO Box 243 Reading RG6 6BB United Kingdom
Tel: +44 (0)118 931 8425 Fax: +44 (0)118 931 8791
www.metoffice.com